Scientific Reports

https://doi.org/10.1038/s41598-026-52648-8

Article in Press

A DPP inhibitor suppresses periodontitis via antibacterial effect targeting *Porphyromonas gingivalis*

Received: 9 December 2025

Accepted: 6 May 2026

Published online: 08 May 2026

Cite this article as: Aoki-Nonaka Y., Minato Y., Hidaka K. *et al.* A DPP inhibitor suppresses periodontitis via antibacterial effect targeting *Porphyromonas gingivalis*. *Sci Rep* (2026). https://doi.org/10.1038/s41598-026-52648-8

Yukari Aoki-Nonaka, Yukako Minato, Koushi Hidaka, Yuko Warita, Daiki Ando, Hnin Yu Lwin, Aoi Matsugishi-Nasu, Naoki Takahashi, Akihiro Nakamura, Wataru Ogasawara, Mizuki Sekiya, Yasumitsu Sakamoto & Koichi Tabeta

We are providing an unedited version of this manuscript to give early access to its findings. Before final publication, the manuscript will undergo further editing. Please note there may be errors present which affect the content, and all legal disclaimers apply.

If this paper is publishing under a Transparent Peer Review model then Peer Review reports will publish with the final article.

ARTICLE IN PRESS

© The Author(s) 2026. **Open Access** This article is licensed under a Creative Commons Attribution-NonCommercial-NoDerivatives 4.0 International License, which permits any non-commercial use, sharing, distribution and reproduction in any medium or format, as long as you give appropriate credit to the original author(s) and the source, provide a link to the Creative Commons licence, and indicate if you modified the licensed material. You do not have permission under this licence to share adapted material derived from this article or parts of it. The images or other third party material in this article are included in the article's Creative Commons licence, unless indicated otherwise in a credit line to the material. If material is not included in the article's Creative Commons licence and your intended use is not permitted by statutory regulation or exceeds the permitted use, you will need to obtain permission directly from the copyright holder. To view a copy of this licence, visit http://creativecommons.org/licenses/by-nc-nd/4.0/.

ARTICLE IN PRESS

A DPP inhibitor suppresses periodontitis via antibacterial effect targeting *Porphyromonas gingivalis*

Yukari Aoki-Nonaka[1,5,†,*], Yukako Minato[1,†], Koushi Hidaka[2], Yuko Warita[1], Daiki Ando[1], Hnin Yu Lwin[1], Aoi Matsugishi-Nasu[1], Naoki Takahashi[1,6], Akihiro Nakamura[3], Wataru Ogasawara[3], Mizuki Sekiya[4], Yasumitsu Sakamoto[4], Koichi Tabeta[1,*]

[1]Division of Periodontology, Faculty of Dentistry & Graduate School of Medical and Dental Sciences, Niigata University, 2-5274 Gakkocho-dori, Chuo-ku, Niigata 951-8514, Japan

[2]Research Facility Center for Science and Technology, Kobe University, 1-1 Rokkodai-cho, Nada-ku, Kobe, Hyogo 657-8501, Japan

[3]Department of Science of Technology Innovation, Nagaoka University of Technology, 1603-1 Kamitomioka, Nagaoka, Niigata 940-2188, Japan

[4]School of Pharmacy, Iwate Medical University, 1-1-1 Idaidori, Yahaba, Iwate 028-3694, Japan

[5]Division of Oral science for Health Promotion, Faculty of Dentistry & Graduate School of Medicine, Dentistry and Health Science, Niigata University, 2-5274 Gakkocho-dori, Chuo-ku, Niigata 951-8514, Japan

[6]Division of Periodontology, Department of Oral Health Science, Hokkaido University Faculty of Dental Medicine, Kita 13, Nishi 7, Kita-ku, Sapporo, Hokkaido, 060-8586, Japan

[†]These authors contributed equally to this work.

[*]Corresponding authors: Y. Aoki-Nonaka and K. Tabeta.

Division of Periodontology, Faculty of Dentistry & Graduate School of Medical

ARTICLE IN PRESS

and Dental Sciences, Niigata University, 2-5274 Gakkocho-dori, Chuo-ku, Niigata 951-8514, Japan.

E-mail: aoki@dent.niigata-u.ac.jp

koichi@dent.niigata-u.ac.jp

Tel: +81-25-227-2871; Fax: +81-25-227-0808

Abstract word count: 198

Total word count: 4482

Number of figures and tables: 5 figures and 1 table

Number of references: 43

Keywords: dipeptidyl peptidase, *Porphyromonas gingivalis,* periodontal disease, antibacterial agents, alveolar bone loss, periodontal medicine

ARTICLE IN PRESS

Abstract

Porphyromonas gingivalis is the most common periodontal pathogen. *P. gingivalis* dipeptidyl peptidase 7 (PgDPP7) belongs to a new class of serine peptidases, family S46. S46 peptidases are absent in mammals. Therefore, these enzymes are promising targets for novel antibacterial agents. In this study, inhibitors were designed based on the cocrystal structures of valyl-tyrosine and phenylalanyl-tyrosine, which bind to the active centers of DPP7 derived from bacteria, and dipeptide derivatives that inhibit PgDPP7 were obtained. The active compound KGDI-109, the first peptidyl inhibitor of S46 peptidases, exerted an inhibitory effect against *P. gingivalis* growth at a minimum inhibitory concentration of 1.56 μM. In C57BL/6N male mice with induced periodontitis, the oral administration of KGDI-109 significantly

ARTICLE IN PRESS

suppressed alveolar bone resorption and reduced the amount of *P. gingivalis* in the oral cavity, indicating that the DPP inhibitor suppresses periodontal disease by its antibacterial activity. This dipeptide derivative did not inhibit the growth of other oral bacteria, and its antibacterial action was presumed to target bacteria possessing DPP, particularly *P. gingivalis*. Furthermore, KGDI-109 may be more effective than AZM in maintaining the gut microbial diversity and reducing adverse health effects. KGDI-109 can be a novel treatment for periodontal diseases targeting *P. gingivalis*.

Introduction

Periodontitis is an inflammatory disease caused by infection with periodontal bacteria, which results in the destruction of periodontal tissues [1]. Among periodontal pathogens, *Porphyromonas gingivalis* has long been regarded as a major causative bacterium due to its virulence factors and its role in severe periodontitis. Hajishengallis et al. proposed that *P. gingivalis* is a keystone bacterium that induces dysbiosis in the oral microbiota, thereby initiating the onset of periodontitis [2,3,4]. However, due to the lack of appropriate tools, its causal role in humans remains unverified. To address this issue and translate the etiological concept to therapeutic strategies, antibiotics specific to *P. gingivalis* could provide direct evidence for its causal role.

P. gingivalis generates its metabolic energy by fermenting amino acids; extracellular oligopeptides are degraded into dipeptides by dipeptidyl

ARTICLE IN PRESS

peptidases (DPPs) [5,6]. These degraded peptides are taken up into the cytoplasm and serve as nutrients essential for *P. gingivalis* growth [7]. DPP7 and DPP11 are members of the S46 exopeptidase family in *P. gingivalis* [8,9]. S46 peptidases are widely distributed in anaerobic Gram-negative species of the genera *Bacteroides*, *Parabacteroides*, and *Porphyromonas,* but they are not found in mammals [9,10]. Antibiotics that target molecules absent in mammals may be associated with a lower risk of side effects; therefore, these peptidases represent promising targets for the development of new antibacterial agents. Sakamoto et al. developed the DPP11 inhibitor SH-5, which exhibits antibacterial activity against *P. gingivalis* [11], but no DPP7 inhibitor has been developed. *P. gingivalis* DPP7 (PgDPP7) is also important for metabolism; therefore, a DPP7 inhibitor could be a specific antibiotic to *P. gingivalis*. Therefore, this study aimed to develop a new peptide-type PgDPP7 inhibitor and investigate its effects on periodontal pathogenic bacteria and its efficacy in preventing periodontal diseases. *P. gingivalis*-specific therapeutics represent an indispensable tool for definitively establishing its causal role in human periodontitis.

Materials and Methods

Reagents

KGDI-109, a DPP7 inhibitor, was synthesized (Figs. S1 and S2). Details regarding reagents are provided in the Supplementary Information.

ARTICLE IN PRESS

Kinetic characterization and inhibition assays

The full nucleotide sequence of the codon-optimized gene and the details on protein production and purification of DPP7 are provided in the Supplemental Materials and Methods and Fig.S3. Protein overproduction and purification were performed as previously described. [12]. The kinetic parameters of purified DPP7 (10 nM) were determined by nonlinear least-squares fitting of the experimental data to the Michaelis–Menten equation using Excel Solver (Microsoft, Redmond, WA, USA), with methionyl-L-leucyl-4-methylcoumaryl-7-amide (1.56, 3.13, 6.25, 12.5, 25, 50, 100, and 200 µM; Met-Leu-MCA; Peptide Institute, Osaka, Japan) as the substrate. The k_{cat} was calculated based on the total protein concentration and reported as an apparent value, as active-site titration was not performed. Inhibition assays were performed using a substrate concentration of 100 µM. Briefly, purified DPP7 (10 nM) was preincubated at 25 °C in a reaction buffer containing 50 mM sodium phosphate (pH 7.0), 5 mM EDTA, 0.005% Tween 20, and various concentrations (1.56–100 µM) of the inhibitor KGDI-109. Reactions were initiated by adding the Met-Leu-MCA substrate (100 µM), followed by continuous fluorescence monitoring every 1 min over 20 min at 25 °C (multipoint kinetic assay). The fluorescence intensity resulting from MCA release was measured using an Infinite 200 PRO microplate reader (Tecan, Männedorf, Switzerland) with excitation at 355 nm and emission at 460 nm. The half-maximal inhibitory concentrations (IC_{50} values) were determined by fitting experimental data from three independent experiments to a three-

ARTICLE IN PRESS

parameter logistic curve (LL.3) using the drc package in R (version 4.3.0) [13]. To account for the technical limitation of the 100 µM maximum inhibitor concentration (imposed by the 1.0% DMSO limit), the bottom plateau of the curve was constrained to zero. The inhibition constants (K_i) were calculated using the Cheng-Prusoff equation [14]. The competitive nature of the inhibition was validated based on the K_i and IC_{50} relationship. Results are reported as the mean with 95% confidence intervals (CI).

Bacterial culture

P. gingivalis W83, *P. gingivalis* ATCC 33277, *Fusobacterium nucleatum* ATCC 25586, and *Prevotella intermedia* ATCC 25611 were cultured in modified Gifu anaerobic medium broth (Nissui, Tokyo, Japan) in an anaerobic jar in the presence of AnaeroPack™ (Thermo Fisher Scientific, Waltham, MA, USA) at 37 °C. *Aggregatibacter actinomycetemcomitans* was cultured in tryptic soy broth supplemented with 6 mg/mL yeast extract and 0.4 mg/mL sodium bicarbonate in an anaerobic jar in the presence of AnaeroPack™ at 37 °C. *Streptococcus mitis* ATCC 903 was cultured in brain heart infusion broth (Thermo Fisher Scientific) at 37 °C under aerobic conditions. The bacterial suspension concentration was determined by measuring the optical density at 600 nm using a UV-visible Spectronic Genesys 10 Bio spectrophotometer (Thermo Fisher Scientific). Colony-forming units (CFU) were standardized using the growth curve of each bacterium [15].

ARTICLE IN PRESS

Inhibition of DPP enzyme activity

P. gingivalis W83 was diluted to 1 × 10^8 CFU/mL, and 100 µL of the cell suspension was transferred to a 96-well plate and incubated with KGDI-109 (0–50 µM) in an anaerobic jar in the presence of AnaeroPack™ at 37 °C for 30 min. Each peptidyl-MCA substrate (PEPTIDE INSTITUTE, INC., Osaka, Japan) was added at 20 µM and incubated for 1 h. The fluorescent emitter produced by hydrolysis of the peptidyl-MCA substrates was measured with excitation at 365 nm and emission at 415–445 nm using GloMax® Explorer (Promega, Madison, WI, USA). Met-Leu-MCA has an amino acid sequence recognized by DPP5 and DPP7 [16, 17], whereas Phe-Met-MCA has an amino acid sequence characteristically recognized by DPP7 [17]. The controls Gly-Pro-MCA and Leu-Asp-MCA have amino acid sequences characteristically recognized by DPP4 and DPP11, respectively [9,16].

Evaluation of the antibacterial activity against oral bacteria

The minimum inhibitory concentration (MIC) and minimum bactericidal concentration (MBC) for KGDI-109 were determined using a microplate dilution assay [15,18]. *P. gingivalis* W83, *F. nucleatum, P. intermedia, A. actinomycetemcomitans*, and *S. mitis* were diluted to 1 × 10^6 CFU/mL, and 100 µL of the cell suspension of each bacterium was transferred to a 96-well plate and incubated in the presence of KGDI-109 (0–200 µM). *P. gingivalis* and *F. nucleatum* were incubated for 72 h, *P. intermedia* was incubated for 48 h, and *A. actinomycetemcomitans* and *S. mitis* were incubated for 24 h. The bacterial suspension concentration was determined by measuring the

ARTICLE IN PRESS

optical density at 600 nm using a UV-visible Spectronic Genesys 10 Bio spectrophotometer (Thermo Fisher Scientific).

For the time-killing assay, *P. gingivalis* W83 was diluted to 1 × 10^8 CFU/mL and treated with KGDI-109 and AZM at 200 μM and AZM at 1.98 μM. The killing curves were determined using the ATP assay (Promega).

Biofilm quantification

P. gingivalis ATCC 33277 was diluted to 1 × 10^8 CFU/mL. The bacterial suspension was transferred into 96-well flat-bottomed plates (Techno Plastic Products AG, Trasadingen, Switzerland) with final KGDI-109 concentrations of 0–200 μM and incubated for 48 h. Biofilm quantification was performed using a crystal violet (Chroma-Gesellschaft Co. Ltd., Münster, Germany) staining method [19].

Cell viability testing

The human monocyte cell line THP-1 (1 × 10^5 cells/well) was incubated for 48 h with 10 ng/mL phorbol 12-myristate 13-acetate (Sigma-Aldrich) in RPMI 1640 medium supplemented with 10% fetal bovine serum (FBS) and 1% penicillin–streptomycin to differentiate macrophage-like cells. The human oral epithelial cell line Ca9-22 (1 × 10^5 cells/well) was cultured in Dulbecco's modified Eagle's medium (Thermo Fisher Scientific) supplemented with 10% FBS and 1% penicillin–streptomycin. These cells were treated with KGDI-109 for 24 h at 37 °C and 5% CO_2. Cell viability was assessed using thiazolyl blue tetrazolium bromide (Sigma-Aldrich). Absorbance was measured at 570 nm using SpectraMax® ABS Plus.

ARTICLE IN PRESS

Mice

Nine-week-old male C57BL/6N/Crl mice (purchased from The Jackson Laboratory Japan, Inc., Kanagawa, Japan) were maintained under specific pathogen-free conditions and fed regular chow. The details are presented in Supplementary Information.

A total of 32 mice were randomly divided into the following groups for the collection of alveolar bone, ligature, and feces samples, as well as body weight data: control group (no-treatment control : nonligation and noninfection), a periodontitis-induced group (periodontitis control : ligation and *P. gingivalis* infection), a KGDI-109-administered periodontitis group (ligation, *P. gingivalis* infection, and KGDI-109 administration), and an AZM-administered periodontitis group (ligation, *P. gingivalis* infection, and AZM administration). Several samples were excluded from the analysis owing to the following reasons: injury, loss of ligature thread, and deficiencies in the sample collection process.

ARTICLE IN PRESS

A total of 16 mice were randomly assigned to the aforementioned groups for a histological analysis of gingival tissue sections. The thread was tied to the mouse under anesthesia, and the mouse was euthanized after the experiment. In this experiment, euthanasia was performed via cervical dislocation under anesthesia before the collection of various samples. Anesthesia was administered via intraperitoneal injection of a mixture of medetomidine (0.3 mg/kg body weight), midazolam (4 mg/kg body weight), and butorphanol tartrate (5 mg/kg body weight) at a dosage of 0.1 mL per

ARTICLE IN PRESS

10 g body weight (mice body weight: 20–25 g at the start of the experiment).

All animal experiments were approved by the Animal Care and Use Committee of Niigata University and conducted in accordance with the Regulations and Guidelines on Scientific and Ethical Care and Use of Laboratory Animals of the Science Council of Japan and the ARRIVE guidelines.

Periodontitis induction in mice and KGDI-109 administration

A 5-0 silk thread was gently ligated around the left maxillary second molar under anesthesia. The threads were kept in place for 7 days. During this period, *P. gingivalis* W83 (2×10^9 CFU), suspended in 200 µL phosphate-buffered saline and 4.5% carboxymethyl cellulose (FUJIFILM Wako Pure Chemical Corporation), was orally administered using a feeding needle once a day to the periodontitis-induced group, whereas the vehicle alone was administered to the control group. KGDI-109 was prepared at a dose of 20 mg/kg body weight in sterile water and administered orally as drinking water.

Alveolar bone resorption quantification

The maxillary bones were stained with 0.5% methylene blue to delineate the cementoenamel junctions and alveolar bone crest. The exposed root area showing alveolar bone resorption surrounded by the cementoenamel junctions and alveolar bone crest of the maxillary second molar was measured using a stereomicroscope (Stemi 305; ZEISS, Jena, Germany)

ARTICLE IN PRESS

[20]. All measurements were performed independently by two masked examiners (HYL and DA).

Histological analysis of periodontal tissue

The maxillae were fixed in 4% paraformaldehyde phosphate buffer solution for 24 h, decalcified in 10% EDTA for 2 weeks, mounted in paraffin, and sectioned at a thickness of 4 μm in the sagittal direction along the long axis of the teeth. The sections were stained with hematoxylin and eosin (H-E; FUJIFILM Wako Pure Chemical Corporation) solutions and a tartrate-resistant acid phosphatase (TRAP) staining kit (Cosmo Bio Corporation, Tokyo, Japan) and imaged using a fluorescence microscope BZ-X710 (KEYENCE, Osaka, Japan). Each image selected for analysis was representative of its group.

Quantification of the bacterial amount

All 5-0 silk threads collected were adjusted to 3 mm in length. Bacterial DNA was isolated using DNeasy Blood & Tissue Kits (QIAGEN, Hilden, Germany). DNA was mixed with PowerUp™ SYBR™ Green Master Mix (Thermo Fisher Scientific) for qPCR and analyzed using QuantStudio™ 1 Real-Time PCR Instrument (Thermo Fisher Scientific). The total bacterial value was assumed to represent the biofilm amount, and normalization was performed by dividing the value for *P. gingivalis* (Δ42-Ct) by the total bacterial value (Δ42-Ct). The oligonucleotides used are shown in Table S1.

Intestinal microflora analysis

The following procedures were performed under contract to Bioengineering

ARTICLE IN PRESS

Lab. Co., Ltd. (Kanagawa, Japan). The details are shown in Supplementary Information. DNA was extracted from the fecal samples. The libraries were prepared using a 2-step tailed PCR method. The primers used are shown in Table S2. The V3/V4 variable region (341f-805r) of the 16S rDNA in the samples was sequenced using the MiSeq system and MiSeq Reagent Kit v3 (Illumina, Inc., San Diego, CA, USA) at 2 × 300 bp. The representative sequences were compared with 97% operational taxonomic units using the Greengene database (version 13_8).

Statistical analysis

Statistical analyses were performed using GraphPad Prism version 7.0 (GraphPad Software, Inc., Boston, MA, USA). The statistical analysis details are shown in the figure legends.

ARTICLE IN PRESS

Results

Design of KGDI-109, a DPP7 inhibitor

The novel dipeptide derivative KGDI-109 is a compound that targets *P. gingivalis* and comprises P2 4-nitro-phenylalanine and P1 *O*-methyltyrosine isopropyl ester (Figure 1a). This design is based on the X-ray cocrystal structure analysis of DPP7, which revealed numerous water molecules in the S1 and S2 pockets interacting with Val-Tyr while leaving unoccupied space [21], and the synthesis of dipeptide analogs with several modifications to the side chains and C-terminus of Val-Tyr and Phe-Tyr [12] targeting *Stenotrophomonas maltophilia* DPP7. KGDI-109 is a modified analog designed based on comparisons of substituents and their functions.

ARTICLE IN PRESS

Specifically, it combines, a P2-substituted phenylalanine, which exhibited strong *P. gingivalis* growth inhibition, with an isopropyl ester at the C-terminal structure, which exhibited low cytotoxicity and stability against human carboxylesterase (Patents JP7228828 and JP7836044). KGDI-109 was synthesized using conventional peptide condensation and deprotection reactions (Fig. S1). Starting with *tert*-butyloxycarbonyl (Boc)-protected *O*-methyltyrosine, the carboxylic acid was converted to an isopropyl ester using 2-bromopropane. After Boc deprotection, the Boc-protected 4-nitro-phenylalanine was coupled using the 1-ethyl-3-(3-dimethylaminopropyl) carbodiimide-1-hydroxybenzotriazole method. The intermediate was purified by flash chromatography, deprotected, and recrystallized to give KGDI-109 as the hydrochloride form in high yield with >98% purity (Fig. S2).

Inhibition of P. gingivalis DPP7 by KGDI-109

The inhibitory effect of KGDI-109 on purified PgDPP7 was investigated. PgDPP7 was produced in *E. coli* and purified by liquid chromatography, resulting in a homogeneous enzyme preparation that showed a single band on SDS–PAGE corresponding to its theoretical molecular weight of 77.8 kDa. The kinetic parameters for Met-Leu-MCA were determined using this purified enzyme, and the k_{cat} and K_m values were 0.197 ± 0.004 s^{-1} and 87.8 ± 2.6 μM, respectively. The IC_{50} and K_i values in inhibition assays with KGDI-109, conducted in the presence of 100 μM substrate, were determined to be 53.8 μM (95% CI: 50.2–57.4) and 25.1 μM (95% CI: 23.5–

ARTICLE IN PRESS

26.8), respectively (Figure 1b). The competitive nature of this inhibition was supported by the design of KGDI-109 as a substrate-mimetic dipeptide analog. Furthermore, it was validated by the kinetic relationship where the K_i value was approximately half of the IC_{50} at a substrate concentration (100 μM) near the K_m (87.8 μM), which is consistent with the theoretical requirement for competitive inhibition.

The specific inhibition of DPP7 enzyme activity by KGDI-109 was evaluated. The fluorescence emission of the MCA substrates designed for each DPP was measured upon bacterial uptake and hydrolysis. KGDI-109 administration inhibited the degradation of DPP7 and DPP5 substrates in a concentration-dependent manner. Furthermore, it exerted a stronger inhibitory effect on the degradation of substrates that react more specifically with DPP7. On the other hand, it did not inhibit the degradation of substrates corresponding to DPP4 and DPP11 (Figure 1c).

ARTICLE IN PRESS

ARTICLE IN PRESS

Figure. 1

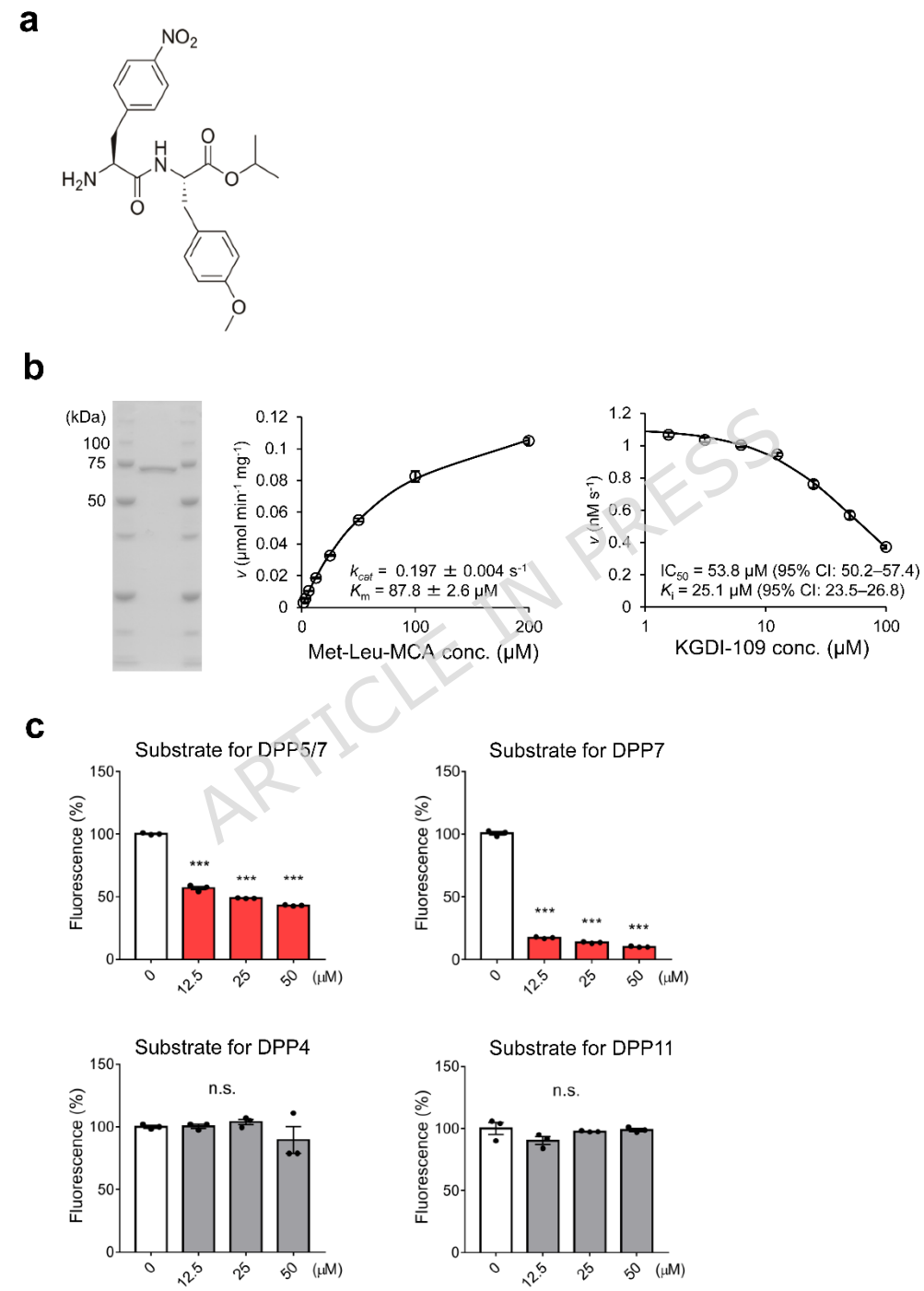

ARTICLE IN PRESS

KGDI-109 exhibited a selective antibacterial effect against P. gingivalis

The MIC and MBC of KGDI-109 were determined to show its antibacterial effects (Table 1). KGDI-109 showed an inhibitory effect against *P. gingivalis* at an MIC of 1.56 μM but did not show an inhibitory effect against *F. nucleatum*, *P. intermedia*, *A. actinomycetemcomitans*, or *Streptococcus mitis*.

Conversely, other antibacterial drugs, such as AZM, ERY, and CHX, showed a broad antibacterial spectrum against all of these bacteria. KGDI-109 was compared with AZM. The growth-inhibitory activity of KGDI-109 against *P. gingivalis* was concentration-dependent (Figure 2a). The antibacterial kinetics study showed that KGDI-109 significantly reduced bacterial ATP activity in a relatively shorter time compared with AZM (Figure 2b). Additionally, KGDI-109 significantly inhibited biofilm formation by *P. gingivalis* (Figure 2c). The cytotoxicity study results are shown in Figure 2d. Ca9-22 and THP-1 cells were exposed to KGDI-109 for 24 h. KGDI-109 at 200 μM did not affect cell viability in either Ca9-22 or THP-1 cells.

ARTICLE IN PRESS

ARTICLE IN PRESS

Figure. 2

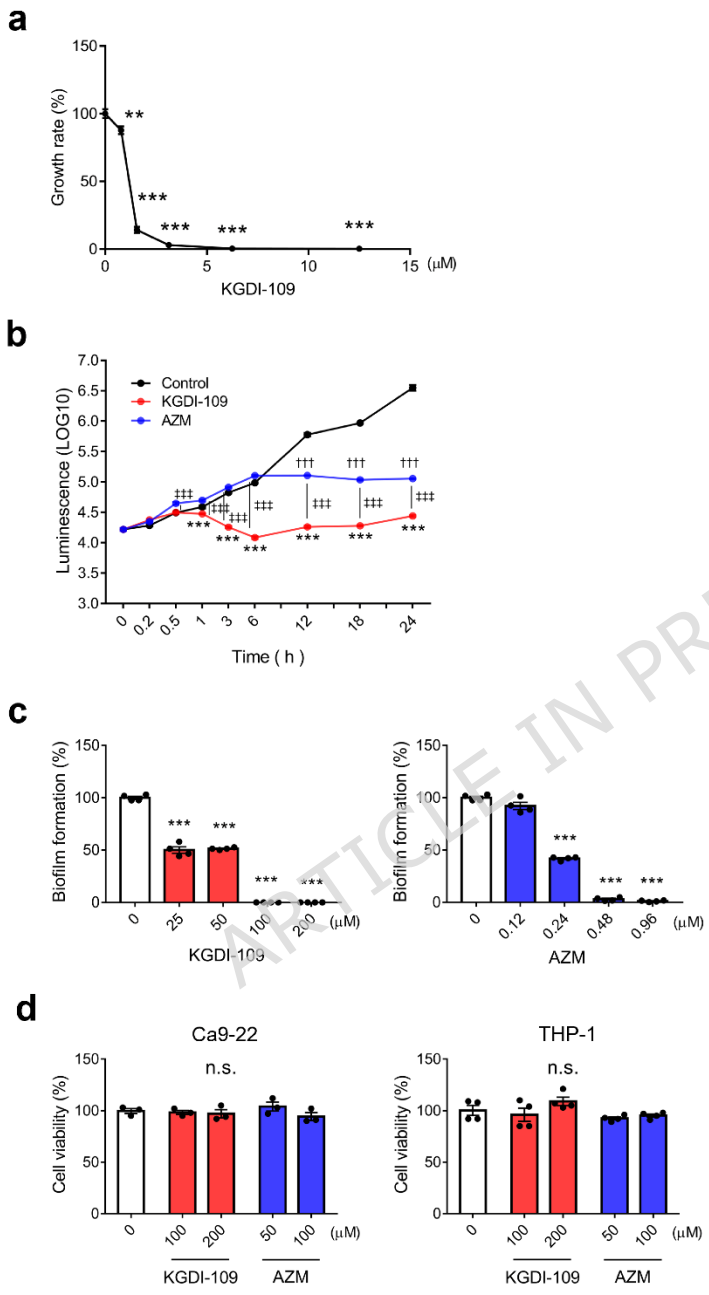

ARTICLE IN PRESS

ARTICLE IN PRESS

KGDI-109 inhibited periodontal tissue destruction in an experimental murine model of periodontitis

The effect of KGDI-109 on periodontal disease was investigated in a mouse model of periodontitis caused by oral *P. gingivalis* infection. No abnormalities in health status or body weight were observed following KGDI-109 administration (Figure 3a). KGDI-109 administration significantly inhibited bone resorption in periodontitis-induced mice (Figures 3b and 3c). In gingival tissue sections stained with H-E, attachment loss was observed in the periodontitis-induced group compared with the control group, and it was suppressed in the KGDI-109-treated group (Figures 3d and 3e). In the same experiment, osteoclast activities in periodontal destruction were assessed by evaluating the number of TRAP-positive cells. The number of TRAP-positive cells adjacent to the bone surface in the interalveolar septa was significantly decreased in KGDI-109-treated mice compared with periodontitis-induced mice (Figures 3f and 3g).

ARTICLE IN PRESS

ARTICLE IN PRESS

Figure. 3

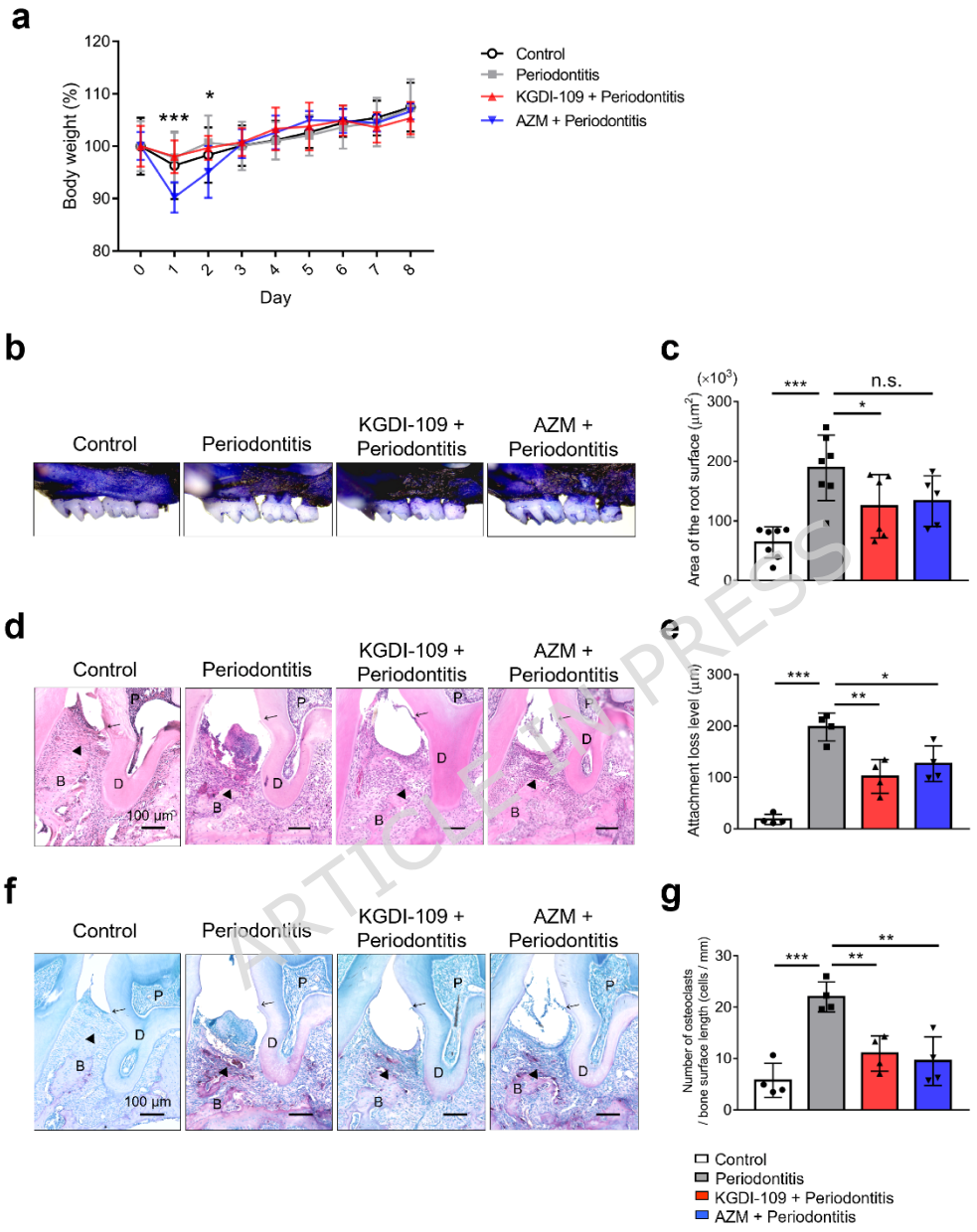

ARTICLE IN PRESS

KGDI-109 reduced the amount of P. gingivalis in the oral cavityand had an effect on the intestinal flora less than that of AZM

The bacterial count in the oral cavity was measured by qPCR after 7 days of KGDI-109 administration to confirm the effectiveness of the specific antibacterial activity of KGDI-109 against *P. gingivalis* in the periodontitis mouse model. The amount of total bacteria in the oral cavity showed no significant change between groups, whereas the amount of *P. gingivalis* was significantly reduced following KGDI-109 treatment (Figure 4a).

The effects of KGDI-109 on the intestinal microbiota were further investigated. Figure 4b presents the relative abundance of intestinal bacterial taxa at the genus level. The AZM group showed a different profile from the other groups. Figure 4c presents the result of alpha diversity analysis conducted to evaluate the microbial community diversity within a sample. Although the AZM group showed a significant decrease in alpha diversity compared with the periodontitis group, the KGDI-109 group showed higher alpha diversity than the periodontitis group (Figure 4c). Furthermore, the AZM group differed greatly from the other groups in composition, whereas the KGDI-109 group had a composition like that of the control group, indicating maintained diversity of the intestinal flora (Figure 4d).

ARTICLE IN PRESS

ARTICLE IN PRESS

Figure. 4

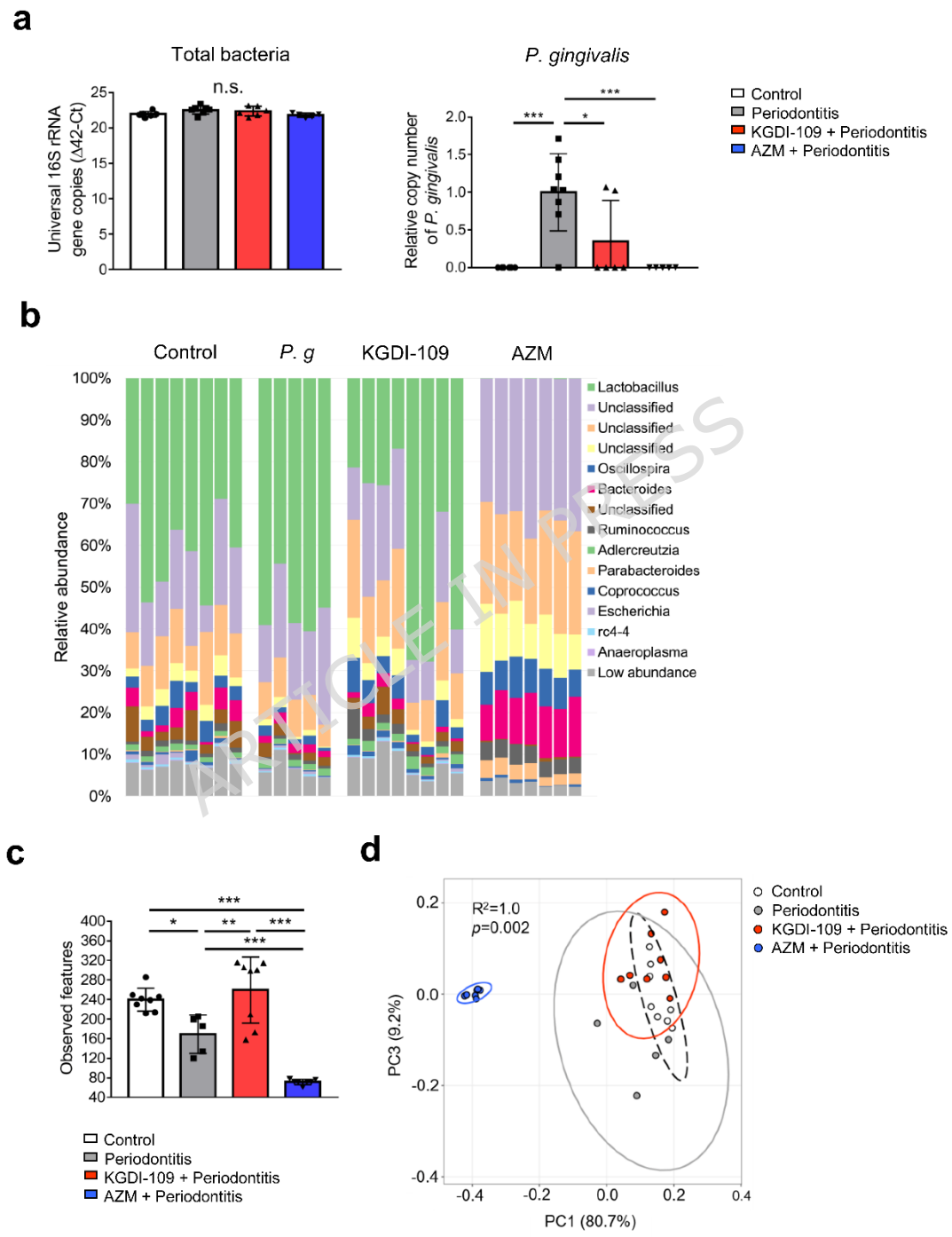

ARTICLE IN PRESS

Discussion

To the best of our knowledge, this is the first study to demonstrate the periodontal disease inhibitory effect of a DPP inhibitor that targets *P. gingivalis*. In this study, inhibitors were designed based on the cocrystal structures of valyl-tyrosine and phenylalanyl-tyrosine, which bind to the active centers of DPP7 derived from bacteria, and the dipeptide derivative KGDI-109 that inhibited PgDPP7 was obtained. The results showed that KGDI-109 inhibited amino acid metabolism by DPP7, thereby depleting the nutrient source necessary for *P. gingivalis* growth.

Oral administration of KGDI-109 significantly suppressed alveolar bone resorption. The amount of *P. gingivalis* in the oral cavity was significantly reduced, indicating that the DPP inhibitor suppresses periodontal disease by its antibacterial activity against *P. gingivalis*. Figure 5 shows an overview of this study.

ARTICLE IN PRESS

P. gingivalis is an asaccharolytic bacterium that degrades proteins via gingipains and DPPs and exclusively utilizes amino acids as an energy source [5,6]. Arginine- and lysine-specific proteinases, RgpA, RgpB, and Kgp [22,23,24], are present in the cell membrane or outer membrane vesicles and among the major virulence factors of *P. gingivalis* [25,26,27]. Extracellular proteins are initially degraded to oligopeptides via gingipains and transported into the periplasmic space [28]. DPPs are localized in the periplasm and degrade oligopeptides to dipeptides or tripeptides [29,30]. As

ARTICLE IN PRESS

this bacterium mainly takes up protein nutrients as dipeptides or tripeptides, DPPs are essential for its survival and proliferation. RgpA, RgpB, and Kgp demonstrate high specificity for the basic amino acid lysine or arginine; thus, KGDI-109, whose S1 subsite structure features hydrophobic side chains, is not expected to strongly bind to gingipains. Figure 1c suggests that KGDI-109 acts as a substrate-competitive inhibitor, particularly for substrates that specifically react with DPP7. DPP7 has been reported to prefer hydrophobic residues at the P1 [8] and P2 [16] positions.

The suppression of alveolar bone resorption by KGDI-109, which likely does not inhibit gingipain activity, is primarily due to bacterial count reduction by the DPP inhibitor, thereby suppressing proliferation. In a periodontitis model in which mice were infected with the *P. gingivalis* W83 strain, metronidazole, which does not directly inhibit gingipain [31], has been shown to suppress alveolar bone resorption [32]. This indicates that reducing the amount of bacteria through antimicrobial effects weakens their pathogenicity. Additionally, even when infecting SPF mice with the W50 strain, which demonstrates strong gingipain activity like W83, no alveolar bone resorption occured [2]. Therefore, the mechanism of periodontal disease induction does not necessarily originate from gingipain.

In previous reports, the triple knockout mutant of DPPIV, DPP-7 and PTP-A indicated a 40% decrease in growth rate in minimal medium GA, whereas the growth of single- and double-knockout mutants was like that of W83

ARTICLE IN PRESS

[33]. The growth of the mutant strain NDP212, which lost *dpp4*, *dpp5, dpp7*, *and dpp11,* was significantly more retarded than the wild type in an anaerobic bacterial culture medium; however, this growth inhibition was limited [29]. The Met-Leu-MCA hydrolysis activity increased in the quadruple-deficient strain (NDP212) compared to the wild type. Such an excessive increase in activity suggests that it is caused by the induction of acylpeptidyl oligopeptidase (PGN_1349) and other unknown peptidases that complement and compensate for the four DPP deficiencies. Furthermore, the DPP11 activity is elevated in gingipain-deficient mutant cells, suggesting that it compensates for the loss of gingipain activity [29]. Elevated DPP4 and PTP-A activities have also been reported in *porT* mutants that do not express functional gingipain [34]. Therefore, the limited growth inhibition observed in the DPP knockout strain [29] [33] suggests that the absence of a specific DPP may be compensated for by other DPP types. Furthermore, gene-deficient strains may have established alternative metabolic pathways optimized for an environment that lacks DPP during repeated proliferation.

ARTICLE IN PRESS

Unlike the limited growth inhibition reported in DPP knockout strains, the pharmacological inhibition by KGDI-109 in this study resulted in a potent growth-inhibitory effect. This may be because the rapid action of the inhibitor may not allow sufficient time for such a compensation or adaptation to occur. Furthermore, the potent growth-inhibitory effect of KGDI-109 may be further enhanced by its ability to simultaneously block

ARTICLE IN PRESS

redundant pathways, as demonstrated by its dose-dependent inhibition of Met-Leu-MCA hydrolysis—a substrate recognized by both DPP5 and DPP7. The MIC may be lower than the IC50 for DPP7 based on the DPP dependence of peptide metabolism in *P. gingivalis* and the potential for KGDI-109 to simultaneously inhibit multiple DPPs. Furthermore, DPPs targeted by KGDI-109 are localized in the periplasmic space. KGDI-109 is highly lipophilic and readily permeates the outer membrane, whereas its inner membrane permeability is low. Consequently, the compound equilibrates across the outer membrane and is localized in the narrow periplasmic space, where the target enzymes may act as a reservoir [35], the total local concentration likely exceeds the MIC, which is the external concentration. Further research is needed to elucidate the detailed mechanism of action of the inhibitor.

ARTICLE IN PRESS

KGDI-109 did not inhibit tumor necrosis factor-α production induced by stimulation with toll-like receptor agonists containing *P. gingivalis* lipopolysaccharide (Fig. S5), indicating that KGDI-109 does not have anti-inflammatory effects. Additionally, KGDI-109 administration reduced the number of TRAP-positive cells in the periodontal tissue of mice. However, it did not have a direct effect on osteoclast differentiation *in vitro* (Fig. S6a). These findings indicate that the inhibition of periodontal tissue destruction and decrease in TRAP-positive cells are the result of inflammatory reaction suppression by the antibacterial activity of KGDI-109. Furthermore, KGDI-109 did not affect osteoblast calcified nodule formation (Fig. S6b). These

ARTICLE IN PRESS

findings indicate that KGDI-109 has no anti-inflammatory or direct effects on bone metabolism and that the inhibition of alveolar bone resorption in the mouse model is due to its specific antibacterial activity against *P. gingivalis.*

In this study, the bacterial load adhering to the ligature was measured by qPCR (Figure 4a). Although AZM has a broad antimicrobial spectrum, the total bacterial did not change. This may be due to the persistence of a certain amount of biofilm formed by oral commensal bacteria around the ligature, even after azithromycin administration, and the potential inclusion of dead bacteria within the biofilm in qPCR results. Antibiotics such as ampicillin and vancomycin have been reported to cause dramatic changes in the abundance and diversity of the gut microbiota. However, they do not have a significant impact on the oral microbiota, indicating that the oral microbiota, characterized by frequent exposure to various environmental factors, is more resilient to antibiotic disruption [36]. Our findings indicate a reduction in *P. gingivalis following* KGDI-109 administration, suggesting that it alters the composition rather than the quantity of the oral biofilm. Future studies are needed to investigate changes in the composition and diversity of the oral microbiota to provide a more detailed understanding of the mechanism of action of KGDI-109.

In this study, *P. gingivalis* infection altered the gut microbiota and reduced bacterial alpha diversity (Figure 4), consistent with previous reports [37]. In

ARTICLE IN PRESS

Figure 4b, the genus *Porphyromonas* was not dominant in the *P. gingivalis*-administered group, likely because *P. gingivalis* does not colonize the gut [37,38]. Even in the absence of intestinal colonization, *P. gingivalis* has been reported to induce ileal inflammation and $IL9^+$ $CD4^+$ lamina propria T cells, thereby impairing the gut epithelial barrier function by inducing dysbiosis of the gut microbiota [37].

The advantages of using a narrow-spectrum antibacterial agent are sparing antibiotic use and curtailing the emergence of resistance [39]. In addition, maintaining beneficial microbiota can prevent complications such as antibiotic-associated diarrhea [39,40]. KGDI-109 exhibited that the change in the intestinal flora was less than that of AZM and that the diversity of the resident bacterial flora was maintained via selective inhibition of *P. gingivalis* (Figure 4). KGDI-109 may be more effective than AZM in maintaining the diversity of lactic acid bacteria, which is essential for maintaining health and reducing adverse health effects. Moreover, clinical evaluation of *P. gingivalis*-specific KGDI-109 will elucidate the etiology of periodontal disease. KGDI-109 may also be beneficial in preventing systemic diseases associated with *P. gingivalis*, such as diabetes and rheumatoid arthritis [41,42].

This study has several limitations. First, the number of bacterial species examined in this study was limited. KGDI-109 may exhibit antibacterial activity against other bacteria if they have DPPs like those of *P. gingivalis*.

ARTICLE IN PRESS

Second, further investigations into the biological stability of KGDI-109 and its clinical administration methods are needed. Heat treatment at 100°C for 10 min did not affect the antibacterial activity of KGDI-109 (Table S3). In addition to the effects of acids and enzymes, considering their behavior in the body, such as their half-life, is necessary. Third, the model used in this experiment has some limitations. Bacterial flora changes and inflammatory bone resorption occur even with ligation alone [43], therefore, investigating the effects of DPP inhibitors in settings other than combined models is necessary. Furthermore, verifying their effects on the human bacterial flora and in periodontitis remains a challenge. Further studies are needed to determine the efficacy and side effects in humans.

ARTICLE IN PRESS

ARTICLE IN PRESS

Figure. 5

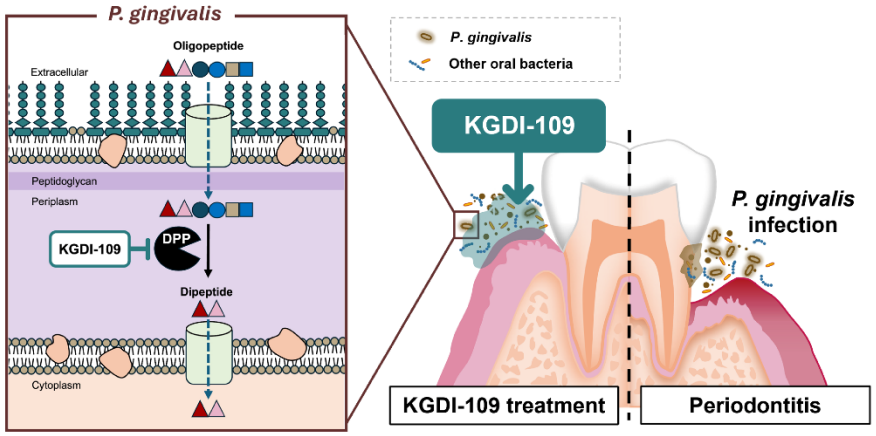

ARTICLE IN PRESS

ARTICLE IN PRESS

Conclusion

KGDI-109, a DPP inhibitor, showed an inhibitory effect against *P. gingivalis* growth and suppressed alveolar bone resorption. KGDI-109 has the potential to be a novel treatment for periodontal diseases, targeting *P. gingivalis* and maintaining gut microbial diversity.

References

1 Pihlstrom, B. L., Michalowicz, B. S. & Johnson, N. W. Periodontal diseases. *Lancet* **366,** 1809-1820 (2005).

2 Hajishengallis, G. et al. Low-abundance biofilm species orchestrates inflammatory periodontal disease through the commensal microbiota and complement. *Cell Host Microbe* **10,** 497-506 (2011).

3 Hajishengallis, G. Immunomicrobial pathogenesis of periodontitis: keystones, pathobionts, and host response. *Trends Immunol.* **35,** 3-11 (2014).

4 Hajishengallis, G., Darveau, R. P. & Curtis, M. A. The keystone-pathogen hypothesis. *Nat. Rev. Microbiol.* **10,** 717-725 (2012).

5 Nemoto, T. K. & Ohara-Nemoto, Y. Dipeptidyl-peptidases: key enzymes producing entry forms of extracellular proteins in asaccharolytic periodontopathic bacterium *Porphyromonas gingivalis*. *Mol. Oral Microbiol.* **36,** 145-156 (2021).

6 Nemoto, T. K. & Ohara-Nemoto, Y. Exopeptidases and gingipains in *Porphyromonas gingivalis* as prerequisites for its amino acid metabolism. *Jpn. Dent. Sci. Rev.* **52,** 22-29, (2016).

7 Nelson, K. E. et al. Complete genome sequence of the oral pathogenic bacterium *Porphyromonas gingivalis* strain W83. *J. Bacteriol.* **185,** 5591-5601, (2003).

8 Banbula, A. et al. *Porphyromonas gingivalis* DPP-7 represents a novel type of dipeptidylpeptidase. *J. Biol. Chem.* **276,** 6299-6305 (2001).

9 Ohara-Nemoto, Y. et al. Asp- and Glu-specific novel dipeptidyl peptidase 11 of *Porphyromonas gingivalis* ensures utilization of proteinaceous energy sources. *J. Biol. Chem.* **286,** 38115-38127 (2011).

10 Suzuki, Y. et al. Identification of the catalytic triad of family S46 exopeptidases, closely related to clan PA endopeptidases. *Sci. Rep.* **4,** 4292 (2014).

11 Sakamoto, Y. et al. Fragment-based discovery of the first nonpeptidyl inhibitor of an S46 family peptidase. *Sci. Rep.* **9,** 13587 (2019).

12 Nakamura, A. et al. Structural basis for an exceptionally strong preference for asparagine residue at the S2 subsite of *Stenotrophomonas maltophilia* dipeptidyl peptidase 7. *Sci. Rep.* **11,** 7929 (2021).

13 R Core Team. _R: A Language and Environment for Statistical Computing_. R Foundation for Statistical Computing, Vienna, Austria. https://www.R-project.org/. (2025).

14 Cheng, Y. & Prusoff, W. H. Relationship between the inhibition constant (K1) and the concentration of inhibitor which causes 50 per cent inhibition (I50) of an enzymatic reaction. *Biochem. Pharmacol.* **22,** 3099-3108 (1973).

ARTICLE IN PRESS

15 Lwin, H. Y. et al. Soybean peptide inhibits the biofilm of periodontopathic bacteria via bactericidal activity. *Arch. Oral Biol.* **142,** 105497 (2022).
16 Rouf, S. M. A. et al. Phenylalanine 664 of dipeptidyl peptidase (DPP) 7 and phenylalanine 671 of DPP11 mediate preference for P2-position hydrophobic residues of a substrate. *FEBS Open Bio* **3,** 177-183 (2013).
17 Nemoto, T. K., Ono, T. & Ohara-Nemoto, Y. Establishment of potent and specific synthetic substrate for dipeptidyl-peptidase 7. *Anal. Biochem.* **548,** 78-81 (2018).
18 Wang, H. Y. et al. Efficacy of a novel antimicrobial peptide against periodontal pathogens in both planktonic and polymicrobial biofilm states. *Acta Biomater.* **25,** 150-161 (2015).
19 Matsugishi, A. et al. Rice peptide with amino acid substitution inhibits biofilm formation by *Porphyromonas gingivalis* and Fusobacterium nucleatum. *Arch. Oral Biol.* **121,** 104956, (2021).
20 Aoki-Nonaka, Y. et al. A peptide derived from rice inhibits alveolar bone resorption via suppression of inflammatory cytokine production. *J. Periodontol* **90,** 1160-1169 (2019).
21 Sakamoto, Y. et al. S46 peptidases are the first exopeptidases to be members of clan PA. *Sci. Rep.* **4,** 4977 (2014).
22 Pavloff, N. et al. Molecular cloning and structural characterization of the Arg-gingipain proteinase of *Porphyromonas gingivalis*. Biosynthesis as a proteinase-adhesin polyprotein. *J. Biol. Chem.* **270,** 1007-1010 (1995).
23 Pavloff, N. et al. Molecular cloning and characterization of *Porphyromonas gingivalis* lysine-specific gingipain. A new member of an emerging family of pathogenic bacterial cysteine proteinases. *J. Biol. Chem.* **270,** 1595-1600 (1997).
24 Scott, C. F., Whitaker, E. J., Hammond, B. F., & Colman, R. W. Purification and characterization of a potent 70-kDa thiol lysyl-proteinase (Lys-gingipain) from *Porphyromonas gingivalis* that cleaves kininogens and fibrinogen. *J. Bio.l Chem.* **268,** 7935-7942 (1993).
25 Fitzpatrick, R. E., Wijeyewickrema, L. C., & Pike, R. N. The gingipains: scissors and glue of the periodontal pathogen. *Porphyromonas gingivalis. Future Microbiol.* **4,** 471-487 (2009).
26 Lunar, S.I. & Cascales, E. Molecular strategies underlying Porphyromonas gingivalis virulence. *J. Mol. Biol*. **433,** 166836 (2021).
27 Curtis, M.A., Garnett, J.A. & Darveau, R.P. The keystone-pathogen hypothesis updated: the role of *Porphyromonas gingivalis* in periodontitis. *J. Periodontal Res.***10,** 70050 (2025).
28 Madej, M. et al. Structural and functional insights into oligopeptide acquisition by the RagAB transporter from *Porphyromonas gingivalis*. *Nat. Microbiol.* **5,** 1016-1025 (2020).
29 Ohara-Nemoto, Y. et al. Identification and characterization of prokaryotic dipeptidyl-peptidase 5 from *Porphyromonas gingivalis*. *J. Bioll. Chem.* ***289*****,** 5436-5448 (2014).
30 Takahashi, N. & Sato, T. Preferential utilization of dipeptides by *Porphyromonas gingivalis*. *J. Dent. Res.* **80,** 1425-1429 (2001).

ARTICLE IN PRESS

31 Bras, G. et al. The efficacy of antimicrobial therapies in the treatment of mixed biofilms formed between *Candida albicans* and *Porphyromonas gingivalis* during epithelial cell infection in the aspiration pneumonia model. *Med. Microbiol. Immunol.* **214,** 8 (2025).

32 Lubcke, P.M. et al. Periodontal treatment prevents arthritis in mice and methotrexate ameliorates periodontal bone loss. *Sci. Rep*. **9**, 8128 (2019).
33 Oda, H., Saiki, K., Tonosaki, M., Yajima, A. & Konishi, K. Participation of the secreted dipeptidyl and tripeptidyl aminopeptidases in asaccharolytic growth of *Porphyromonas gingivalis*. *J. Periodontal Res*. **44,** 362-367 (2009).
34 Nguyen, K-A. et al. Verification of a topology model of PorT as an integral outer-membrane protein in *Porphyromonas gingivalis. Microbiology* **155,** 328-337 (2009).

35 Pandeya, A. et al. Periplasmic targets for the development of effective antimicrobials against Gram-negative bacteria. *ACS Infect. Dis*.**6,** 2337-2354 (2020).
36 Wu, H. et al. Antibiotic-induced dysbiosis of the rat oral and gut microbiota and resistance to Salmonella. Arch. Oral. Biol. **114,** 104730 (2020).
37 Sohn, J. et al. *Porphyromonas gingivalis* indirectly elicits intestinal inflammation by altering the gut microbiota and disrupting epithelial barrier function through IL9-producing $CD4^+$ T cells. *Mol. Oral Microbiol.* **37,** 42-52 (2022).
38 Geva-Zatorsky, N. et al. Mining the human gut microbiota for immunomodulatory organisms. *Cell* **168,** 928-943. E11 (2017).
39 Alm, R. A. & Lahiri, S. D. Narrow-spectrum antibacterial agents-benefits and challenges. *Antibiotics* **9,** 418 (2020).
40 McFarland, L. V. Epidemiology, risk factors and treatments for antibiotic-associated diarrhea. *Dig. Dis.* **16,** 292-307 (1998).
41 Ohtsu, A. et al. Influence of *Porphyromonas gingivalis* in gut microbiota of streptozotocin-induced diabetic mice. *Oral Dis.* **25,** 868-880 (2019).
42 Sato, K. et al. Aggravation of collagen-induced arthritis by orally administered *Porphyromonas gingivalis* through modulation of the gut microbiota and gut immune system. *Sci. Rep.* **7,** 6955 (2017).

43 Matsuda, Y. et al. Ligature-induced periodontitis in mice induces elevated levels of circulating interleukin-6 but shows only weak effects on adipose and liver tissues. *J Periodontal Res.* **51**, 639-646 (2016).

Author Contributions

Y. A-N., Y. M., and K. H. contributed to conception, design, data acquisition, analysis, and interpretation and drafted and critically revised the manuscript. Y. W., D. A., H. Y-L., A. M-N., and M. S. contributed to data acquisition and analysis and critically revised the manuscript. N. T. and W. O. contributed to data interpretation and critically revised the manuscript. A. N. contributed to

ARTICLE IN PRESS

design, data acquisition, analysis, and interpretation and drafted and critically revised the manuscript. Y. S. contributed to conception and interpretation and critically revised the manuscript. K. T. contributed to data interpretation and drafted and critically revised the manuscript. All authors gave their final approval and agree to be accountable for all aspects of the work.

Data availability

The data that support the findings of this study are available from the corresponding author, upon reasonable request.

Competing interest

The authors declare no competing interests.

ARTICLE IN PRESS

Funding

The authors disclosed receipt of the following financial support for the research, authorship, and publication of this article: This work was supported by the Japan Society for the Promotion of Science (JSPS, Tokyo, Japan) KAKENHI [grant numbers JP24K12945 and JP21K09913 to Y. A-N.] and the Adaptable and Seamless Technology Transfer Program through Target-Driven R&D (A-STEP) from the Japan Science and Technology Agency [grant number JPMJTM20FL to K.-H.].

Ethics approval

Protocols for animal experiments were approved by the Animal Care and Use Committee of Niigata University (approval nos. SA00626, SA01326, SA01515, SA01274, and SA01172) on March 17, 2020, and conducted in

ARTICLE IN PRESS

accordance with the Regulations and Guidelines on Scientific and Ethical Care and Use of Laboratory Animals of the Science Council of Japan and the ARRIVE guidelines.

All animal housing and experiments were conducted in strict accordance with the institutional Guidelines for Care and Use of Laboratory Animals at Niigata University.

Figure Legends

Figure 1. Development of the DPP7 peptide inhibitor. (**a**) Chemical structure of KGDI-109. (**b**) Characterization and inhibition assay using purified PgDPP7. SDS–PAGE analysis of purified PgDPP7, showing a single band corresponding to the theoretical molecular weight of 77.8 kDa (left). Purified enzyme (2 µg) was subjected to SDS–PAGE using a 10% acrylamide gel; a representative cropped image is shown, and the original, full-length gel image is provided in Supplementary Figure S4. Michaelis–Menten plot of PgDPP7 activity against the Met-Leu-MCA substrate (center). Inhibition curves of PgDPP7 activity by KGDI-109 in the presence of 100 µM substrate (right). Error bars represent the standard deviations from three independent experiments. IC_{50} and K_i and values represent the 95% CI from three independent experiments. (**c**) Inhibition of DPP7 enzyme activity by KGDI-109 in *P. gingivalis*. The fluorescent emitter produced by the hydrolysis of the peptidyl-MCA substrates was measured ($n = 3$). *P. gingivalis* was preincubated with KGDI-109 (0–50 µM), and the peptidyl-MCA substrates were added at 20 µM and incubated for 1 h. The peptidyl-

ARTICLE IN PRESS

MCA substrates, Met-Leu-MCA, Phe-Met-MCA, Gly-Pro-MCA, and Leu-Asp-MCA, are shown in the figure as substrates for DPP5/7, DPP7, DPP4, and DPP11, respectively.

Data are presented as means ± SD from three independent experiments. Significant values are indicated by $^{***}P < 0.001$ vs. 0 μg/mL. Comparisons were performed using Dunnett's multiple comparison test.

Figure 2. KGDI-109 had an antibacterial effect against *P. gingivalis*. (**a**) Growth rate of *P. gingivalis* with KGDI-109. The rate was calculated for each sample using the following formula: (average OD value of sample − average OD value of medium) / (average OD value of control − average OD value of medium) × 100. *P. gingivalis* was diluted to 1×10^6 CFU/mL and treated with 0–100 μM KGDI-109 for 72 h ($n = 3$). Significant values are indicated by $^{**}P < 0.01$ and $^{***}P < 0.001$, vs. 0 μg/mL. (**b**) The antibacterial kinetics of KGDI-109. *P. gingivalis* was diluted to 1×10^8 CFU/mL and treated with KGDI-109 at 200 μM and AZM at 1.98 μM for 0–24 h ($n = 4$). Significant values are indicated by $^{***}P < 0.001$ (control vs. KGDI-109), $^{\dagger\dagger\dagger}P < 0.001$ (control vs. AZM), and $^{\ddagger\ddagger\ddagger}P < 0.001$ (KGDI-109 vs. AZM). Comparisons were performed using Dunnett's multiple comparison test. (**c**) The inhibition of biofilm formation by KGDI-109 or AZM against *P. gingivalis*. The remaining amount of biofilm was evaluated using crystal violet staining ($n = 4$). (**d**) Cell viability test. Ca9-22 and THP-1 were treated with KGDI-109 for 24 h and analyzed using the thiazolyl blue tetrazolium bromide assay (Ca9-22: $n = 3$; THP-1: $n = 4$). Data are presented as means

ARTICLE IN PRESS

± SD. Comparisons were performed using Dunnett's multiple comparison test. Significant values are indicated by $^{*}P < 0.05$, $^{**}P < 0.01$, and $^{***}P < 0.001$, vs. 0 μg/mL. n.s. = not significant. Three repeated experiments were conducted.

Figure 3. KGDI-109 inhibited alveolar bone destruction in an experimental murine model of periodontitis. (**a**) Change in body weight. The change in body weight is expressed as a percentage, and the average weight is set as 100% for each group at the start of the experiment. Data are presented as means ± SD. Significant values are indicated as $^{*}P < 0.05$ and $^{***}P < 0.001$ (the AZM group vs. the periodontitis group). (**b**) Representative stereomicroscope images of the maxillae from each group. (**c**) Quantification of alveolar bone destruction: measurement of the exposed root surface area. Data are presented as means ± SD (control: $n = 7$, periodontitis: $n = 7$, KGDI-109-periodontitis: $n = 6$, and AZM-periodontitis: $n = 5$). (**d**) Histological findings of gingival tissue sections stained with H-E. (**e**) Quantification of attachment loss level. The attachment loss level was measured in each section as the distance from the cementoenamel junctions to the gingival margin of the distal first and mesial second molars in the maxilla. Data are presented as means ± SD ($n = 4$). (**f**) Representative TRAP staining images of the interalveolar septal region. (**g**) The number of TRAP-positive osteoclasts (N.Oc) per millimeter of the alveolar bone surface (BS) was measured using ImageJ 1.53t software ($n = 4$). Scale bars = 100 μm. Black arrows indicate the locations of the cementoenamel junctions, and

ARTICLE IN PRESS

black triangles indicate the locations of the alveolar bone crest. B = bone, D = dentin, and P = pulp. Comparisons were performed using Dunnett's multiple comparison test. Significant values are indicated as $^{*}P < 0.05$, $^{**}P < 0.01$, and $^{***}P < 0.001$, vs. the periodontitis group. Three repeated experiments were conducted.

Figure 4. The effects of KGDI-109 on bacteria in the oral cavity and intestine. (**a**) The amount of bacteria in the oral cavity. The Ct values of the universal 16S rDNA and *P. gingivalis* genes from the ligature samples were analyzed using qPCR. The relative quantity of *P. gingivalis* was normalized to that of total bacterial gene copies, the ratio of periodontitis group as 1. Data are presented as means ± SD (control: $n = 6$, periodontitis: $n = 7$, KGDI-109-periodontitis: $n = 6$, and AZM-periodontitis: $n = 5$). Significant values are indicated as $^{*}P < 0.05$ and $^{**}P < 0.01$ (Dunnett's multiple comparison test). n.s. = not significant. Three repeated experiments were conducted. (**b**) The following number of mice were used for the analysis of the intestinal microbiota (control: $n = 8$, periodontitis: $n = 5$, KGDI-109-periodontitis: $n = 8$, and AZM-periodontitis: $n = 7$). Relative abundance of intestinal bacterial taxa at the genus level in each experimental group. (**c**) Bar graphs and dot plots of alpha diversity based on observed features. Data are presented as means ± SD. Significant values are indicated as $^{*}P < 0.05$, $^{**}P < 0.01$, and $^{***}P < 0.001$ (Tukey's multiple comparison test). (**d**) Principal coordinate analysis score plot of the intestinal microbiota profiles of the four groups using unweighted UniFrac distance. $P = 0.002$, for the AZM group vs. the

ARTICLE IN PRESS

control group (analysis of similarity test).

Figure 5. An overview of this study. KGDI-109, a DPP inhibitor, showed an antibacterial effect targeting *P. gingivalis* via inhibition of amino acid metabolism. KGDI-109 is a new antibacterial agent that suppresses periodontitis.

Table 1. MIC and MBC Values.

(μM)	KGDI-109		AZM		ERY		CHX	
	MIC	MBC	MIC	MBC	MIC	MBC	MIC	MBC
Porphyromonas gingivalis	1.56	6.25	0.39	0.39	0.2	0.39	8.8	8.8
Fusobacterium nucleatum	>200	>200	0.39	0.78	12.5	50	70	70
Prevotella intermedia	>200	>200	0.1	0.2	0.1	0.1	35	35
Aggregatibacter actinomycetemcomitans	>200	>200	0.2	0.78	0.39	1.56	17.5	17.5
Streptococcus mitis	>200	>200	0.2	3.13	0.05	1.56	70	70

AZM, azithromycin; ERY, erythromycin; CHX, chlorhexidine; MIC, minimum inhibitory concentration; MBC, minimum bactericidal concentration.

ARTICLE IN PRESS

ARTICLE IN PRESS

Figure. 1

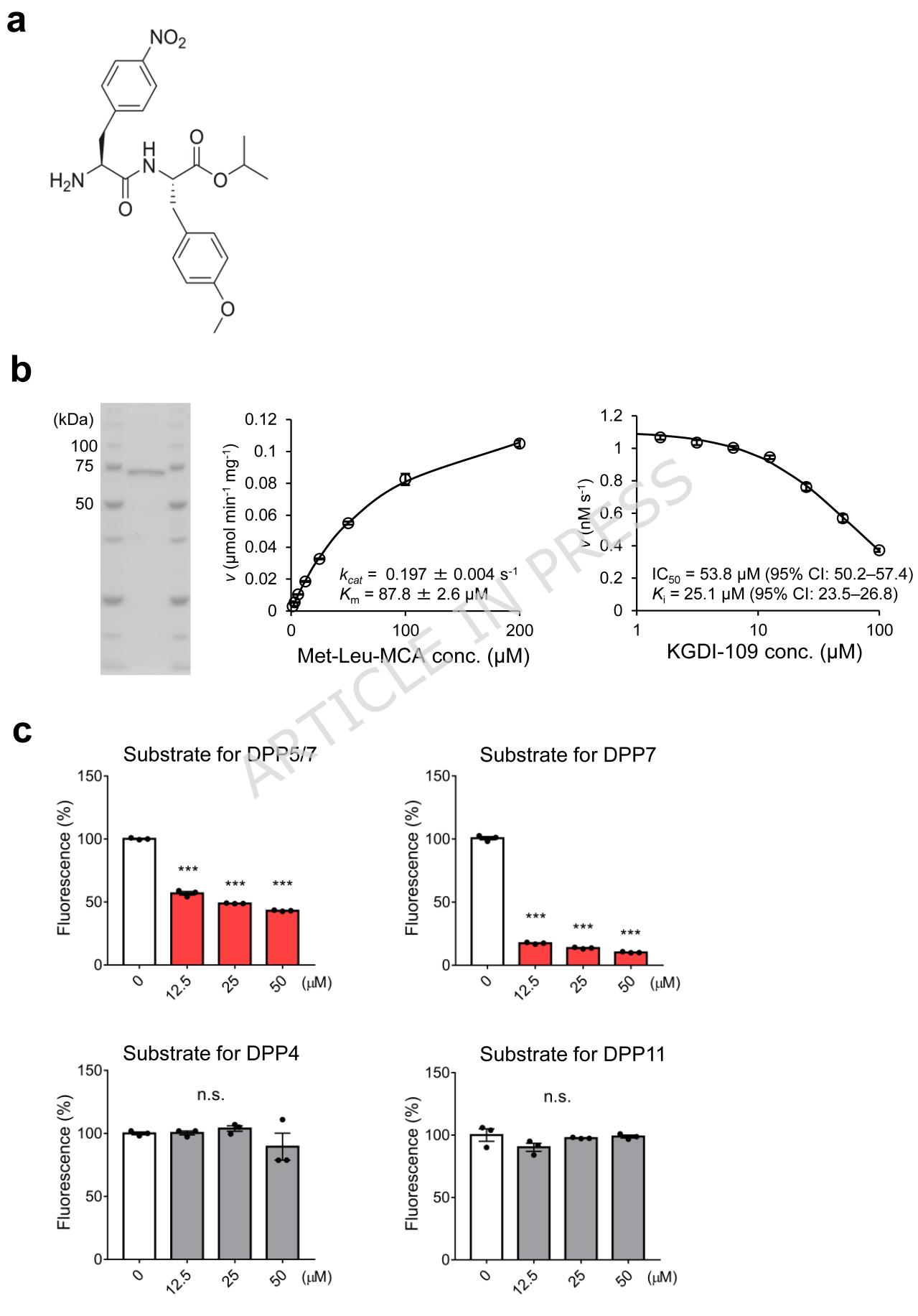

ARTICLE IN PRESS

Figure. 2

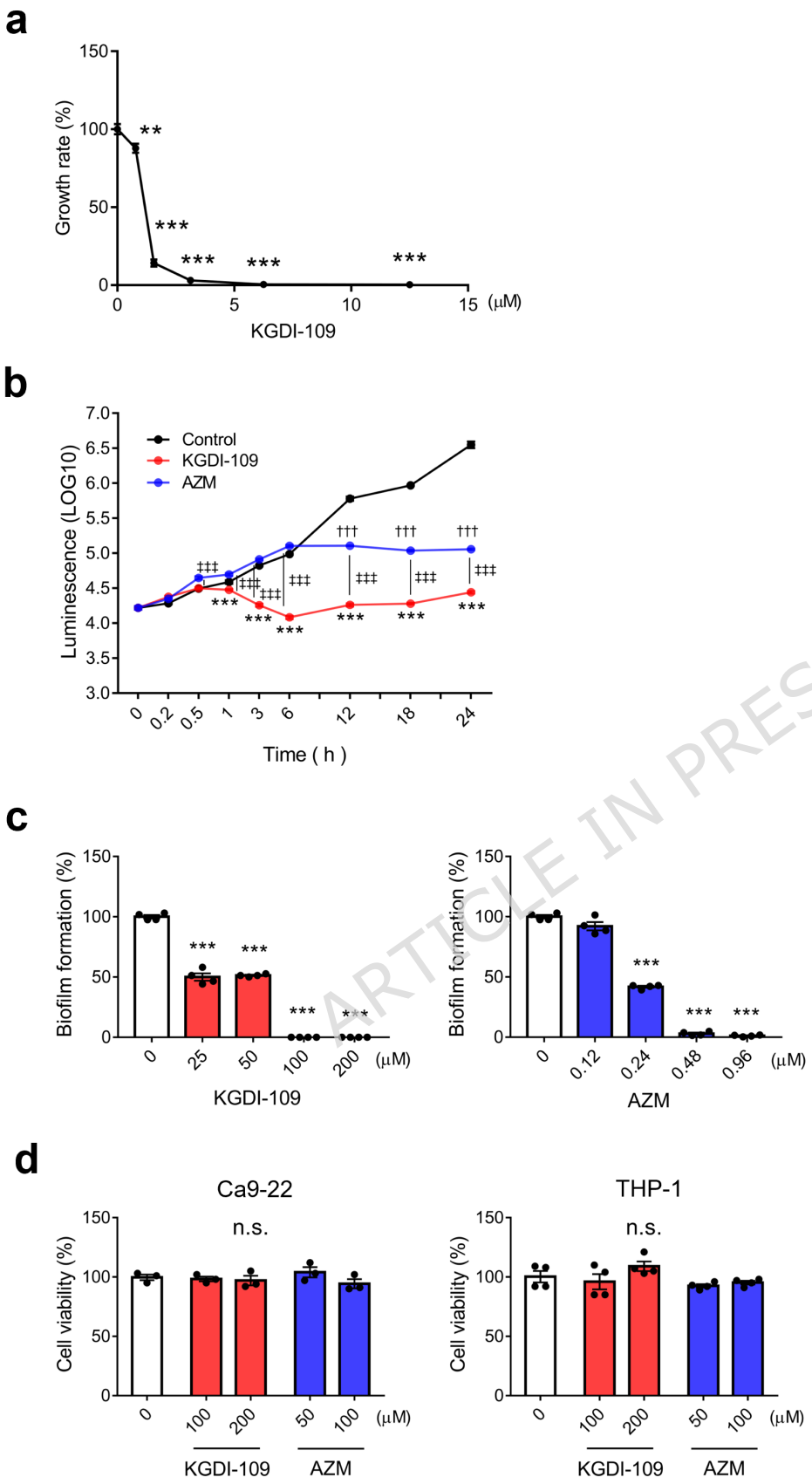

ARTICLE IN PRESS

ARTICLE IN PRESS

Figure. 3

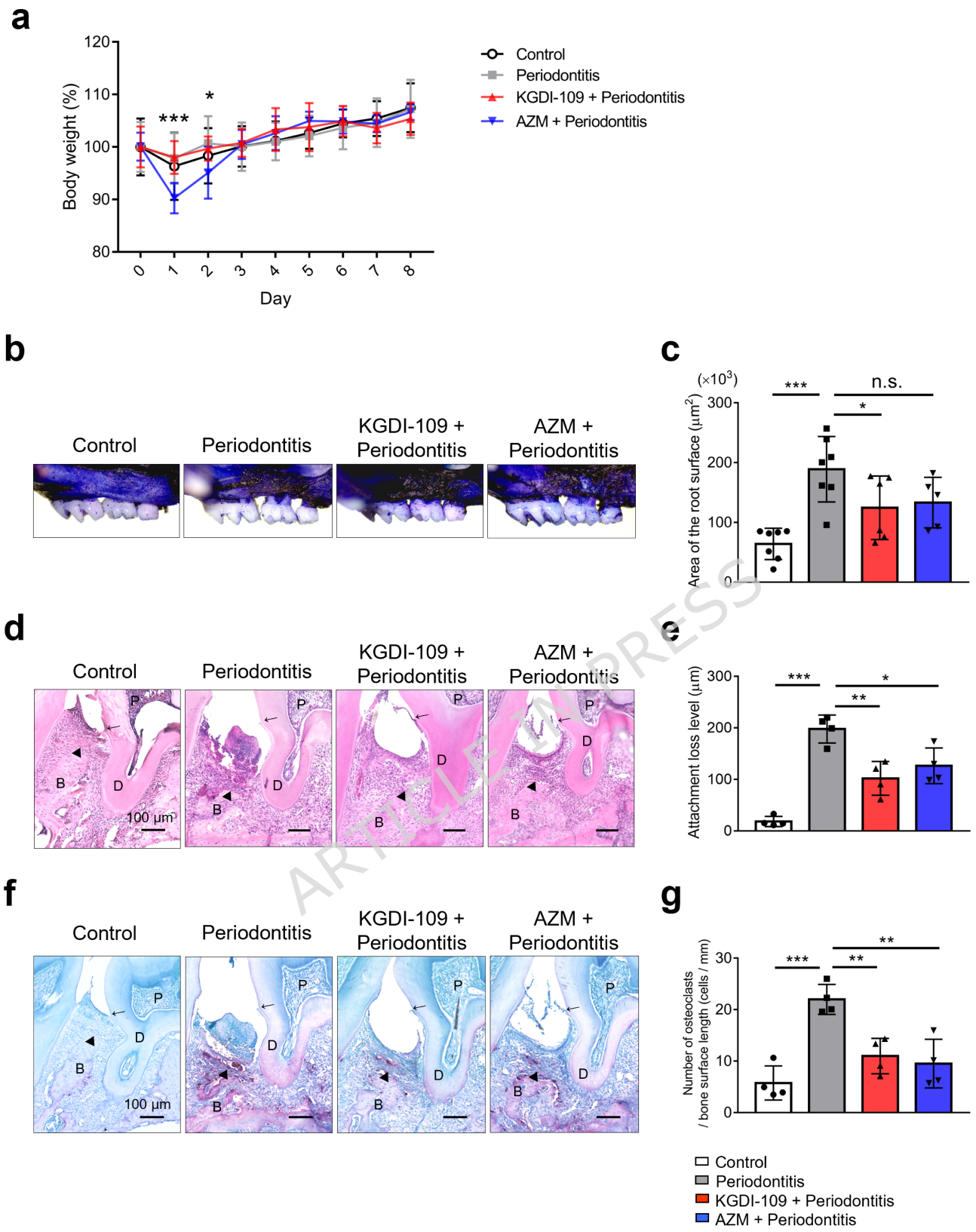

ARTICLE IN PRESS

ARTICLE IN PRESS

Figure. 4

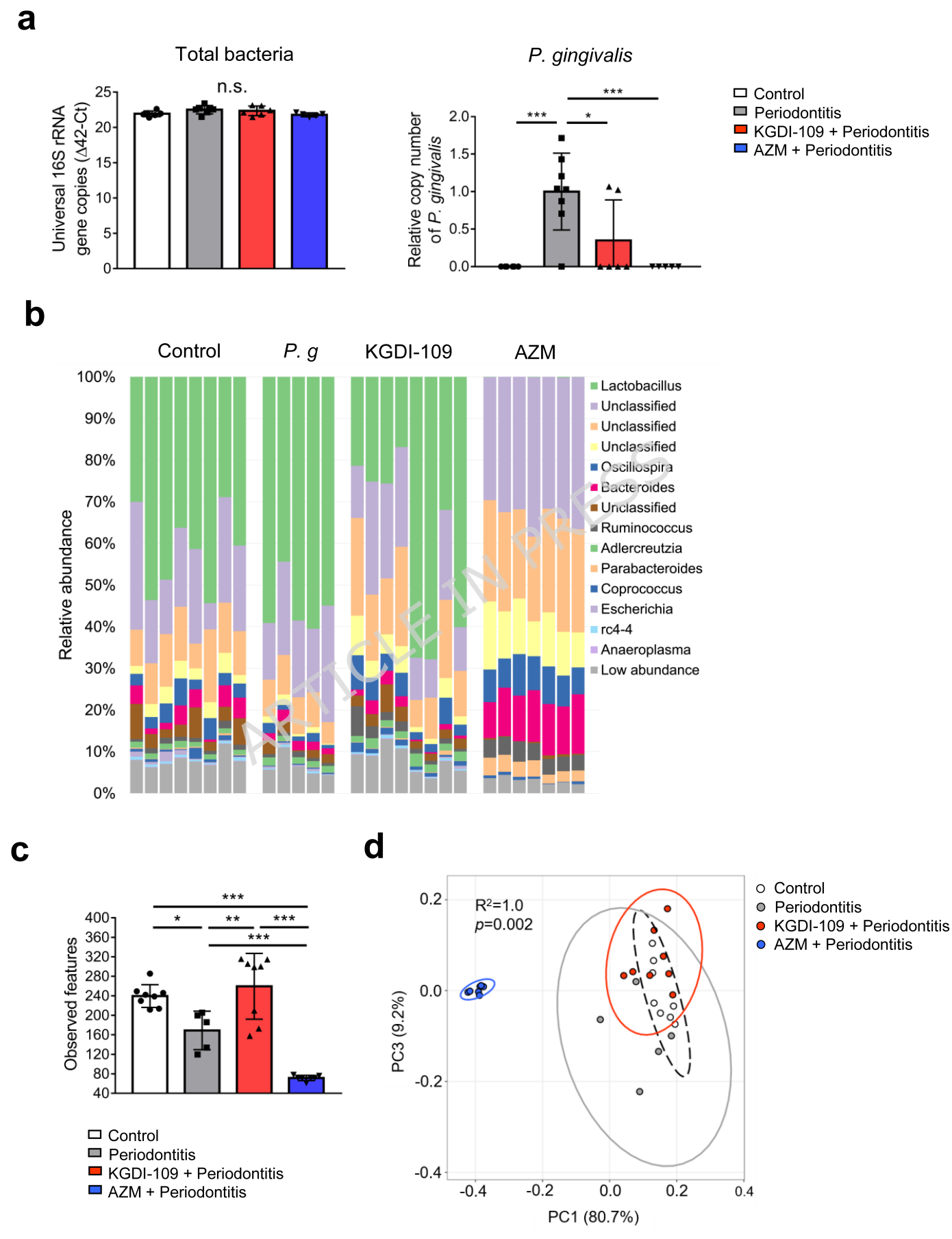

ARTICLE IN PRESS

Figure. 5

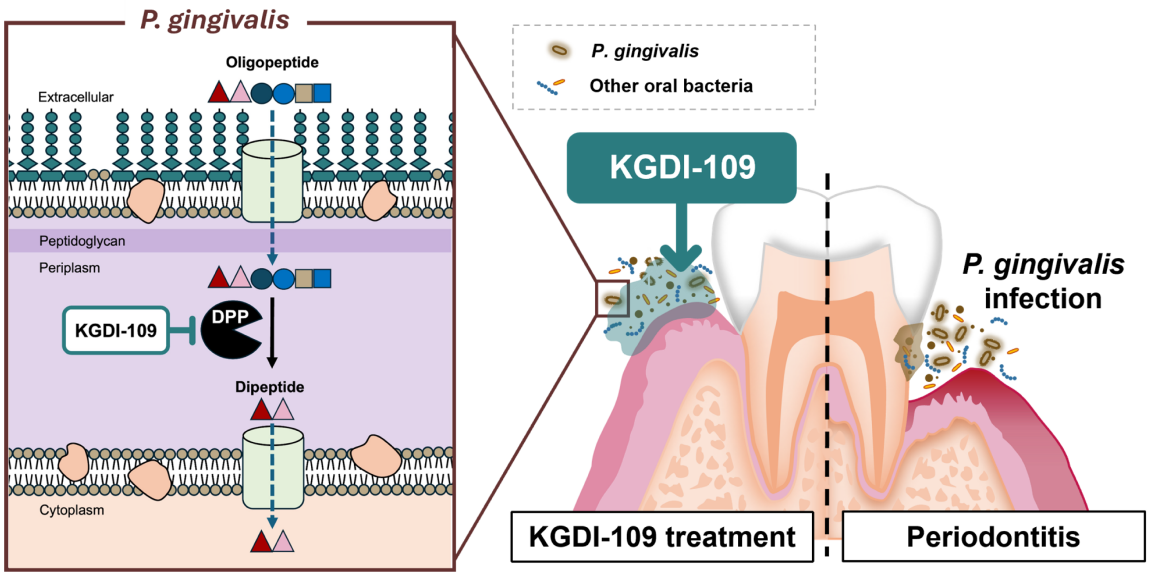

ARTICLE IN PRESS

ARTICLE IN PRESS

Table 1. MIC and MBC Values.

(μM)	KGDI-109		AZM		ERY		CHX	
	MIC	MBC	MIC	MBC	MIC	MBC	MIC	MBC
Porphyromonas gingivalis	1.56	6.25	0.39	0.39	0.2	0.39	8.8	8.8
Fusobacterium nucleatum	>200	>200	0.39	0.78	12.5	50	70	70
Prevotella intermedia	>200	>200	0.1	0.2	0.1	0.1	35	35
Aggregatibacter actinomycetemcomitans	>200	>200	0.2	0.78	0.39	1.56	17.5	17.5
Streptococcus mitis	>200	>200	0.2	3.13	0.05	1.56	70	70

AZM, azithromycin; ERY, erythromycin; CHX, chlorhexidine; MIC, minimum inhibitory concentration; MBC, minimum bactericidal concentration.

ARTICLE IN PRESS